

Hard X-ray Micro-Analysis (HXMA) Beamline 06ID-1

N. Chen, C.-Y. Kim, and W.-F. Chen
Canadian Light Source Inc.

BEAMLINE STAFF:

N. Chen, *scientist*
ning.chen@lightsource.ca
306-657-3571

C.-Y. Kim, *scientist*
chang-yong.kim@lightsource.ca
306-657-3765

W.-F. Chen, *science associate*
weifeng.chen@lightsource.ca
306-657-3829

BEAMLINE TEAM LEADER:

D-T. Jiang
detong@physics.uoguelph.ca
519-824-4120 ext 53982

Beamline Overview

Status	Operational for XAFS, powder diffraction, and microprobe (imaging and XANES) endstations
Source	Superconducting wiggler, $E_c = 10.6$ keV
BL Optics	pre-mono collimating mirror cryogenically cooled DCM Si(111) & Si(220) post-mono toroidal mirror
Energy range	5 – 40 keV
Resolution	1.5×10^{-4} , $\Delta E/E$ (10 keV)
Spot size	1×2.5 mm ² (XAFS) 6×6 μ m ² (microprobe)
Flux (10 KeV)	10^{12} ph/s (XAFS) 10^{10} ph/s (microprobe)

As a fully operational general purpose hard X-ray spectroscopy facility, the CLS 06ID-1 Hard X-ray Micro-Analysis Beamline (HXMA) is sourced by a 1.9 T wiggler with XAFS, microprobe, and diffraction capabilities [1]. The fixed-exit hard X-ray beam is delivered to three endstations at the HXMA SOE by the double crystal monochromator, equipped with Si(111) and Si(220), covering the energy range from 5 to 40 keV. The beamline operates under mirror-mono-mirror mode with either Rh or Pt mirrors in the X-ray beam path for an operation range of 5 to 30 keV, or under mono-only mode between 30 to 40 keV.

Beamline performance

Monochromator Energy Calibration Stability

The monochromator energy calibration stability has been evaluated under mirror-mono-mirror operation mode with the Si(220)/Pt configuration and the beamline wiggler source running at 1.9 T. The testing was performed between two storage injections to cover a complete thermal power loading fluctuation cycle on the beamline optics in the HXMA primary optical enclosure (POE). Cu metallic foil was used as the reference material in the testing. The scan step-sizes used were 10 eV/step, 0.25 eV/step, and 0.1 \AA^{-1} /step for the pre-edge, XANES and post-edge regions, respectively (Figure 1). The mono second crystal was detuned 50 % at the end of the XANES scan range before the collection of each single scan data set. The first inflection point (E_0) of the Cu K-edge XANES spectrum was used as the index for the energy calibration stability (Figure 2). The measurement was

performed by using straight ion chambers in transmission mode. Some experimental details are summarized in Table 1.

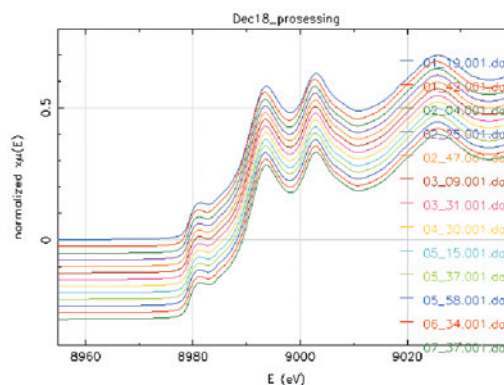


Figure 1: XANES spectra, Cu K-edge. Single scan for each data trace.

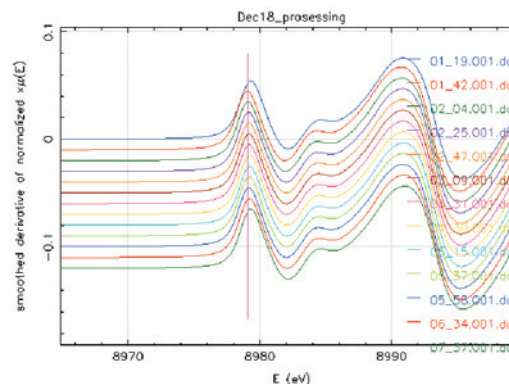


Figure 2: The first derivative spectra of the XANES data of Fig. 1. The vertical bar indicates the stabilized (thermal equilibrated) mono energy position.

Figure 3 displays the correlation between the monochromator energy calibration and the storage ring current, indicating that E_0 drifting follows an unsymmetrical “U” shape trace, composed of a high current (I_{ring}) wing, a plateau region and low current (I_{ring}) wing. The high current wing covers ~ 30 minutes of time directly after storage ring injection. Within this wing the ring current decayed by ~ 7 mA, and E_0 drifted 0.85 eV with a drifting slope of 1.2×10^{-1} (eV/mA). In the plateau region when the ring current is between 244 and 184 eV, E_0 is essentially constant with a drifting slope of 4.6×10^{-4} (eV/mA) at an average value of 8979.16 (± 0.03) eV with a fit residual sum of squares of 0.01 eV². After the plateau region, the E_0 drifting cycle finishes in the low current wing, which starts when the ring current decays to 180 mA. In this

region, the E_0 drifting slope is 1.5×10^{-2} (eV/mA)—two orders of magnitude larger than that of plateau region but 10 times smaller than that of the high current wing.

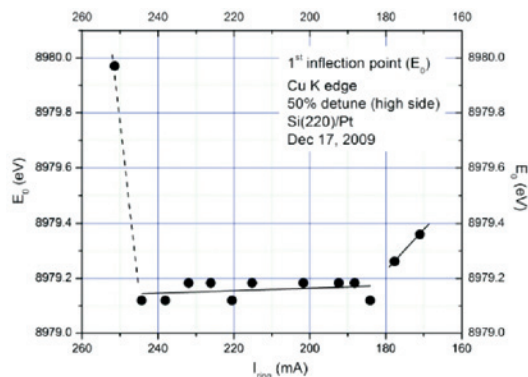


Figure 3: The three regions for the monochromator energy stability versus ring current (I_{ring}), i.e., high current wing (dashed line), plateau region, and low current wing. Notice that since there is not enough data for the high current wing, the trend of the ring is extrapolated based on only two data points, hence presented as a dashed line only.

HXMA's monochromator energy calibration is stabilized a half hour after the storage ring injection, and the energy calibration remains stable for a ring current range of ~ 244 to 184 mA in the 250 mA operation mode. Based on this testing, it is concluded that shortening the injection time, improving the storage ring electron beam lift time, and introducing top-up injection mode (or injection with the front-end shutters open) will improve monochromator performance at HXMA.

Microprobe Compound Focusing

HXMA's microprobe endstation uses a compound focusing system that takes moderately focused beam from a toroidal mirror as a secondary source for the KB mirrors. The compound focusing allows easy control of the KB-focused beam size through adjusting the size of the secondary source using slits. Compound focusing can be achieved in two different ways, putting the secondary source (toroidal focal point) before or after the KB mirrors - HXMA uses the compound focusing scheme with the horizontal focal point behind the KB mirrors. Figure 4 shows measured flux under compound focusing conditions with a $6 \mu\text{m} \times 6 \mu\text{m}$ beam size.

Compound focusing in the microprobe endstation provides greater photon flux than focusing in monochromator-only mode. A detailed study of controlling the KB focused beam size by changing the secondary source slits will be performed in the future.

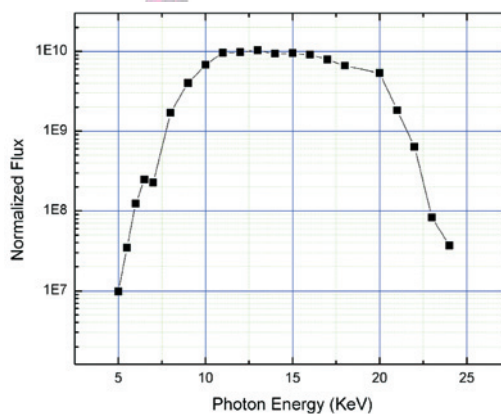


Figure 4: Flux measured at the microprobe station under compound focusing with beam size of $6 \mu\text{m} \times 6 \mu\text{m}$. The focusing was achieved with Rh coated KB mirrors in combination of Si(111) monochromator, Pt-coated toroidal mirror and white beam slit size of 1 mm x 4 mm. The flux was normalized to 250 mA ring current.

New capacities at Psi-8 Diffractometer

Both an ARS cryostat (10 K – 450 K) and Rayonix CCD165 are now available for the general user program. Macros for temperature control of cryostat and CCD image acquisition have been incorporated into the SPEC software. Figure 5 shows a grazing incidence X-ray scattering image from a diblock copolymer film.

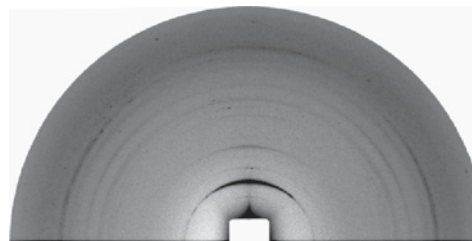


Figure 5: CCD image of grazing incident X-ray diffraction measurement from a diblock co-polymer thin film. Courtesy of Xavier Roy (UBC).

References

1. Jiang, T. D., Chen, N., and Sheng W., 2009, p800. Wiggler-based Hard X-ray spectroscopy beamline at CLS, AIP Proc. 879 (Accelerators and Beams), 800-803.